An Acad Bras Cienc (2023) 95(Suppl. 3): e20220652 DOI 10.1590/0001-3765202320220652
Anais da Academia Brasileira de Ciências | *Annals of the Brazilian Academy of Sciences*
Printed ISSN 0001-3765 I Online ISSN 1678-2690
www.scielo.br/aabc | www.fb.com/aabcjournal

GEOSCIENCES

Ocean-atmosphere turbulent CO_2 fluxes at Drake Passage and Bransfield Strait

CELINA CÂNDIDA F. RODRIGUES, MARCELO F. SANTINI, LUCIANA S. LIMA, MYLENE J. CABRERA, ELIANA B. ROSA, UESLEI ADRIANO SUTIL, JONAS T. CARVALHO, JACOB W. BURNS & LUCIANO P. PEZZI

Abstract: The oceans play an important role in mitigating climate change by acting as large carbon sinks, especially at high latitude regions. The Southern Ocean plays a major role in the global carbon dioxide (CO_2) budget. This work aims to investigate the behavior of turbulent CO_2 fluxes and quantify it under different atmospheric and oceanic conditions in the Drake Passage and Bransfield Strait regions on high spatiotemporal resolutions when compared with traditional CO_2 fluxes estimations. The atmospheric stability condition was used to corroborate the description of CO_2 fluxes. *In situ*, satellite, and reanalysis data from 08 to 22 November 2018, were used in this work. The Bransfield Strait uptaked 38.59% more CO_2 than the Drake Passage due to the cold and fresh waters, allied to the influence of glacial meltwater dilution. Which increased the CO_2 solubility, directing the CO_2 fluxes to the ocean. The Bransfield Strait had predominantly stable atmospheric conditions, which contributed to this region acting as a CO_2 sink. The Drake Passage, on average, behaved as a CO_2 sink, mainly due to physical characteristics. This research contributes to a better understanding of the Southern Ocean's role in the global carbon balance on scales that are very difficult to monitor.

Key words: carbon flux, sea-air interaction, carbon sinks, Antarctic Peninsula.

INTRODUCTION

The main cause of global warming, according to the Intergovernmental Panel on Climate Change (IPCC) (IPCC 2021), is the increase of greenhouse gases (GHG) emissions in the atmosphere since the pre-industrial period. Carbon dioxide (CO_2), one of the most important GHG, has increased by over 40% since the pre-industrial period. These values increased from 278 ppm in 1750 to 411.97 ppm in 2019, and the average global air temperature increased 0.89 °C between the years 1880 and 2019 (NOAA 2019).

Relevant scientific questions about global climate involve the understanding of the interaction between the ocean and atmosphere (Pezzi et al. 2009, 2016, 2021, Hackerott et al. 2018, Santini et al. 2020, Souza et al. 2021). According to Canadell et al. (2007), the oceans are responsible for sequestering approximately 1/3 of anthropogenic carbon emissions per year. The CO_2 partial pressure in the ocean (pCO_{2sw}) has great spatial and temporal variability, being middle and high latitude regions considered CO_2 sinks (Takahashi et al. 2009). The high latitudes have an important role in CO_2 exchange between ocean-atmosphere, which in turn are controlled by physical, chemical, and biogeochemical processes (Ito et al. 2018, Monteiro et al. 2020, Jiang et al. 2014).

Recent studies show that the Southern Ocean (SO) plays a major role in the global CO_2 cycle, accounting for 43% (42 Pg C) of the global anthropogenic CO_2 uptake from the atmosphere from 1870 to 1995 (Takahashi et al. 2009, Frölicher et al. 2015, Le Quéré et al. 2016, 2018). The SO sinks more CO_2 during the spring-summer than the autumn-winter due mainly to the sea-ice cover retreats and biologically driven (Roden et al. 2016, Ito et al. 2018, Ogundare et al. 2021).

Several modelling and observational studies suggest a reduction in the efficiency of SO CO_2 uptake over the past few decades (Lovenduski et al. 2013, 2015, Le Quéré et al. 2010, Metzl 2009). Nevertheless, other studies suggest that global ocean uptake of CO_2 has increased over the past decade, largely due to the SO (Landschützer et al. 2014, Majkut et al. 2014, Munro et al. 2015, Xue et al. 2015). There is a need for studies that allow a better understanding of the processes involved in the exchange between the ocean and the atmosphere, at different spatiotemporal scales. Understanding how CO_2 turbulent flux behaves in different oceanic regions is very important for global carbon budget studies. The Atlantic Carbon and Fluxes Experiment (ACEx) project (Pezzi et al. 2016), the Ocean-Atmosphere Interaction Program in the Brazil-Malvinas Confluence Region (INTERCONF) (Pezzi et al. 2005, 2009), Southern Ocean Studies for Understanding Global Climate Issues (SOS-CLIMATE; Orselli et al. 2017, Ito et al. 2018, Monteiro et al. 2020), Programme de Coopération avec l'Argentine pour l'e´tude de l'océan Atlantique Austral (ARGAU cruises; Bianchi et al. 2009) and more recently the Antarctic Modeling Observation System (ATMOS) project (Pezzi et al. 2021), are some of the South America research programs dedicated to study the exchange of ocean-atmosphere turbulent fluxes in the Southwest Atlantic Ocean (SAO) and the SO.

The observations in the Drake Passage (DP) show higher pCO_{2sw} values located in the north of the Antarctic Polar Front (PF) than to the south (Munro et al. 2015). Additionally, the seasonal cycle amplitude north of the front is much larger and well defined than south of the front. In the south of the PF has been a persistent CO_2 sink, due to the pCO_{2sw} being lower than the CO_2 partial pressure in the atmosphere (pCO_{2atm}) (Caetano et al. 2020), influenced by the cold sea surface temperature (SST) during the summer and the presence of the upwelling of waters with low anthropogenic CO_2 content (Pardo et al. 2014) and mixed layer depths greater in winter (Stephenson et al. 2012). The upwelling of old and CO_2 rich waters around Antarctica influences the carbonate system in the NAP environments (Lencina-Avila et al. 2018, Monteiro et al. 2020). It increases the macronutrients and CO_2 and decrease the carbonate concentration; however, those changes vary depending on mixing processes in response to sea ice, eddies formation, topography, and atmospheric forces (Henley et al. 2019). At the Northern Antarctic Peninsula, the coastal waters of the straits and bays are considered the most productive areas in the SO (Costa et al. 2020). However, according to Caetano et al. (2020), the Bransfield Strait (BS) in late spring indicates a near-neutral air-sea CO_2 flux with a slight source to the atmosphere. Those authors suggest the temperature-sensitive metabolic and physical-chemical process cause significant impact on the spatial distribution of pCO_{2sw} at the BS.

Due to the major role in understanding climate, the biogeochemical cycles, the global energy balance, mass and energy fluxes are important study fields (Trenberth et al. 2009, Takahashi et al. 2009, Le Quéré et al. 2018, Fay et al. 2018). Changes in energy and mass fluxes between the ocean and atmosphere are controlled mainly by wind speed, air and sea temperature, humidity, radiation and evaporation (Sato 2005). The SO provides major contributions to maintaining our planet's climate and plays an important role in the nutrient distribution to other oceans basins (Fay et al. 2018). However, due to its distance and hostility and adverse nature, it is difficult to collect *in situ* data (Pezzi et al. 2021, Monteiro et al. 2020). *In situ* data is typically collected in the summer because the complex environment for experimentation. Therefore, the utilization of satellite data have been complement the in situ data, which help to improve our knowledge of the role of the SO in the global climate (Shutler et al. 2016, Benallal et al. 2017, Wannikhoff & Triñanes 2017, Lohrenz et al. 2018).

The main objective of this work is to investigate the behavior of CO_2 fluxes at the Drake Passage and the Bransfield Strait west coastal areas under different atmospheric and oceanic conditions, during the Spring of 2018 on high spatiotemporal resolutions when compared with traditional CO_2 fluxes estimations. This article is outlined as follows: the section Materials and Methods presents the study area and the experimental design. The Results and Discussion section brings the results and discussion. We finish this article by presenting the conclusions.

MATERIALS AND METHODS

Study area

The main oceanic structure in the SO is the Antarctic Circumpolar Current. It is characterized by strong flows eastward that connect all ocean basins and is responsible for distributing physical and biogeochemical properties around the world (Orsi et al. 1995, Rintoul et al. 2001, Ito et al. 2018). The SO is characterized by extreme winds, strong meridional temperature gradients, and high variability of seasonal climate (e.g. sea ice cover; Swart et al. 2019).

The study region analyzed here is the Atlantic sector of the SO, comprising DP and BS at the east coastal region of the South Shetland Islands. They are in the northwest region of the Antarctic Peninsula and are influenced by waters coming from the southeast sector of DP, BS and the Weddell Sea (WS). The DP comprises the Subantartic front (SAF), Polar Front (PF), South Antarctic circumpolar front (SACCF), and southern boundary (SBdy, Figure 1). The region that goes from the Antarctic continent to the PF is the Antarctic Zone, and the region between the PF and the Subtropical Front is the Subantarctic Zone (Orsi et al. 1995).

The BS encompasses a transition zone between the Bellingshausen Sea and the WS. According to Lopez et al. (1999) this strait is mainly controlled by the interaction of two different fluxes: (i) the warmer and less saline waters from the Bellingshausen Sea (which enters on passages further west at South Shetland Islands) and (ii) the colder and more saline waters from the WS (which enters near the Joinville island). The frontal structure results from the meeting of these two currents, named the Bransfield Front. The BS also is influenced by Antarctic Circumpolar Current that promotes intrusions of Circumpolar Deep Water associated to climatic modes (Barllet et al. 2018). The DP waters also enter at BS, but stay near to the South Shetland Islands, and their interference at BS is negligible (Zhou et al. 2002). Our study area includes the DP and BS as seen in Figure 1.

Observed data

The data sets used here were collected by a micrometeorological tower installed on the bow of the Brazilian Navy Polar Vessel (Po/V) Almirante Maximiano (H41) during the Antarctic Operation 37 (OP37) between 08 to 22 November 2018. This oceanographic cruise is part of the activities planned and developed by the Studies Center of Ocean-Atmosphere-Cryosphere Interaction (CInt) supported by the National Institute for Cryosphere Technology Science that meets the objectives of the ATMOS Project. Those projects surged as a response to a Brazilian Antarctic Program (PROANTAR) scientific call.

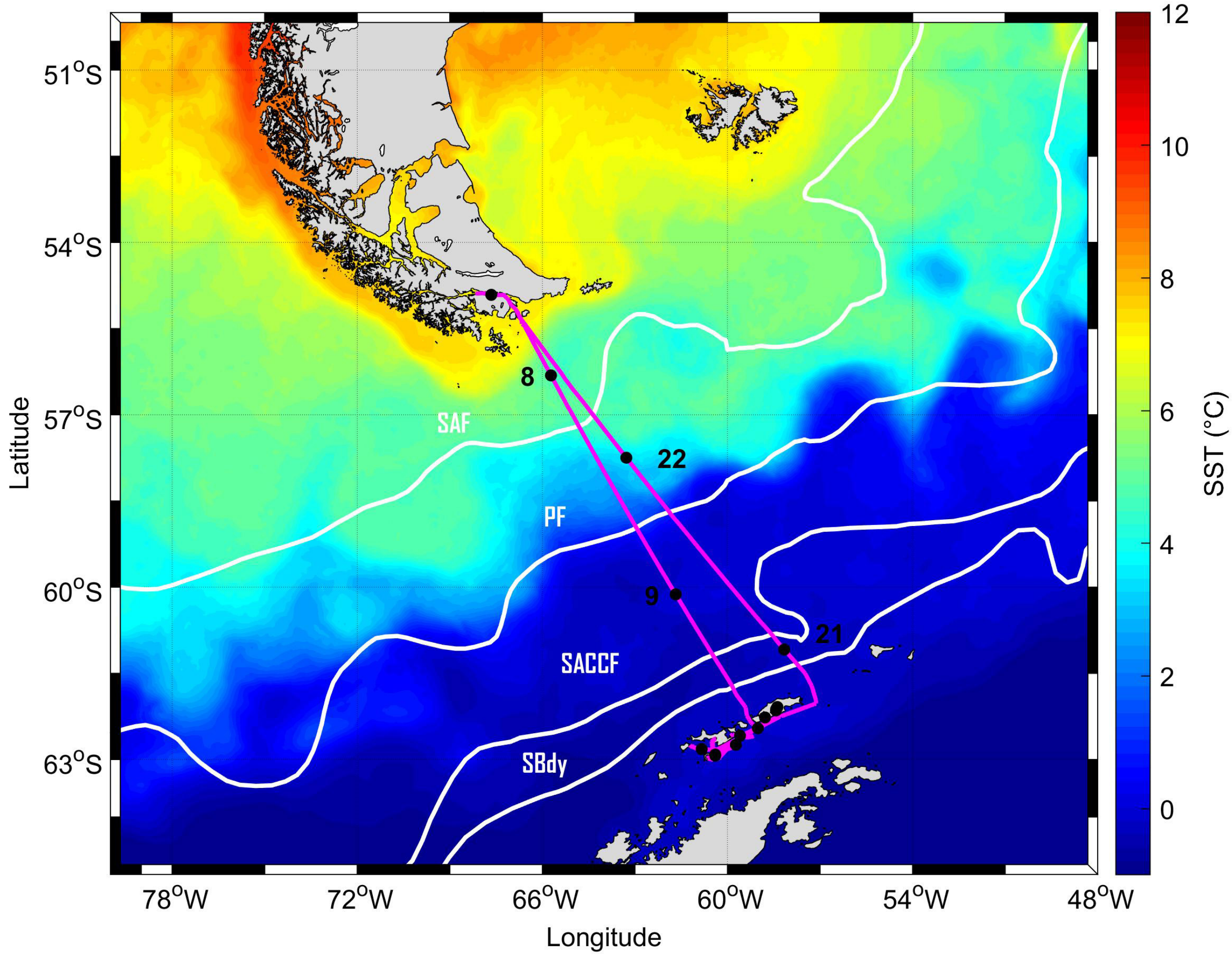

Figure 1. Route of the Brazilian Navy Polar Vessel (Po/V) Almirante Maximiano (H41) and study area. Composite for the period between November 08 to 22 November 2018, Sea surface temperature (°C) derived from Multi-scale Ultra-high Resolution (MUR). White lines: Subantarctic front (SAF), polar front (PF), South Antarctic circumpolar front (SACCF), and southern boundary (SBdy) are frontal positions as defined by Orsi et al. (1995)

The ship tracks are illustrated in Figure 1 and are overlaid on the sea surface temperature (SST) field, which highlights the intense along track SST gradients, characteristic of the Antarctic Circumpolar Current (Orsi et al. 1995). The H41 and micrometeorological tower used in the campaign are shown in Figure 2. The micrometeorological tower was installed approximately 16 m above sea level with a similar setup used in previous cruises in the Southwestern Atlantic (Pezzi et al. 2016, Oliveira et al. 2019, Santini et al. 2020, Souza et al. 2021). More recently this same setup was used in an oceanic mesoscale eddy turbulent flux study at Brazil-Malvinas Confluence (BMC) by Pezzi et al. (2021).

For direct CO_2 turbulent fluxes measurements, in the ocean-atmosphere interface, were used micrometeorological sensors sampling in high-frequency rate (20 Hz; Table I). The sensors included a three-dimensional Sonic Anemometer with an integrated CO_2/H_2O Gas Analyzer (IRGASON, Campbell Scientific, Inc., Logan, UT, USA), a 3-axis IMU (MotionPak 2, Systron Donner), a magnetic compass

Figure 2. Brazilian Navy Polar Vessel (Po/V) Almirante Maximiano (H41) with its micrometeorological tower during the OP37, between 08 to 22 November 2018.

(KVH C100) and a Garmin GPS (GPS16X). The three-dimensional (3-D) linear accelerations, angular rates and geographical position of the ships were measured at the same frequency as the primary measurements used for computing the CO_2 fluxes. The sonic anemometer was fixed in a 1 m long metal bar installed perpendicularly to the vertical mechanical structure of the micrometeorological towers and forward to the ship's bows. This configuration allowed measurements to avoid the flow distortions of the ships' structure on the vertical component of the wind vector (Santini et al. 2020).

The tower sensors were tested and calibrated by the Meteorological Instrumentation Laboratory of INPE before and after the experiment. The Infrared Gas Analyzer (IRGA) is calibrated following the manual instructions (Campbell Scientific 2016) using two different gas concentrations of CO_2, and zero humidity concentration and dew point temperature for the H_2O. The first part of the procedure simply measures the CO_2 and H_2O zero and span, without making adjustments. This allows the CO_2 and H_2O gain factors to be calculated. These gain factors quantify the state of the analyzer before the zero-and-span procedure and were used to correct recent measurements for drift. The last part of the zero-and-span procedure adjusts internal processing parameters to correct subsequent measurements. For zero we used the Analytical Nitrogen 5.0 with minimum purity of the 99.999% to CO_2 and H_20. The

Table I. Description of the sensors installed in the micrometeorological tower, during the OP37, between 08 to 22 November 2018.

Data Source (sampling frequency)	Sensor / Manufacturer	Meteorological Variable
Micrometeorological Tower (20 Hz)	3D Sonic Anemometer and Gas Analyzer (IRGASON/CAMPBELL)	CO_2 concentration (mg m^{-3}); H_20 concentration (g m^{-3}); u, v e w (m/s);
	Motion Pack II/ Systron Donner	Angular velocity (deg s^{-2}); Acceleration (m s^{-2})
Micrometeorological Tower (0.06 Hz)	PT101/CAMPBELL	Atmospheric pressure (hPa)
	HC2S3/VAISALA	Air temperature (°C); Relative humidity (%)
Micrometeorological Tower (20 Hz)	GPS/Garmin	Ship heading (°) Ship velocity (m/s)

CO_2 SPAN was obtained using N_2 balanced CO_2 at a concentration of 396.45 +/- 0.05ppm. The H_2O SPAN was obtained using a Li-Cor LI-610, with the accuracy of ± 0.2 °C dew point.

Unlike traditional measurements performed for oceanic and atmospheric pCO_2 monitoring, where a closed path IRGA (i.e. LI7000 Licor Biogeosciences) was used, we used an open path sensor (IRGASON, Campbell Scientific), where its optical cells were exposed. Closed path sensors require more frequent calibration and quality control than open path sensors. In addition, because the gas needs to travel a path to reach the optical cell, it loses turbulent frequencies compromising the quality of the CO_2 and H_20 fluxes (Fratini et al. 2012). The IRGASON, according to the manufacturer's manual (Campbell Scientific 2016), has a monthly calibration recommendation, a period shorter than the duration of our experiment. The calibration before and after the field campaign was sufficient to maintain the quality of the sampled data. In order to reduce the influence of salt and dust accumulation on the IRGASON optical cells, periodic cleaning of its cells was performed at least weekly. During the processing of the high frequency data, we followed the quality check proposed by Foken et al. (2005).

Eddy Covariance method

The Eddy Covariance (EC) method is based on the covariance between vertical wind components and the gas concentration in the near surface of the atmosphere, which was used to determine turbulent fluxes of mass and heat (Arya 2001, Stull 1988). The EC method measures the covariance between the turbulent fluctuations around their mean and to the dry air density mean during a determined sample interval. The CO_2 flux $\left(F_{CO_2}\right)$ is mathematically defined by Equation 1.

$$F_{CO_2} = \overline{\rho a \, w'c'} \tag{1}$$

where F_{CO_2} is the CO_2 flux in μmol m^{-2} s^{-1}, the bars correspond to the means and the apostrophes indicate the turbulent fluctuations around the mean; ρa is the dry air density (kg m^{-3}), w' is the vertical wind component (m s^{-1}), c' is the ratio of CO_2 to dry air density (μmol mol^{-1}).

Wind data sampled by mobile platforms need corrections to remove the influence of ship movements. The spurious fluctuations caused by these movements must be removed, with the methodology applied by Edson et al. (1998) and Miller et al. (2008) originally based on Fujitani (1981). A detailed description of the wind data correction to remove ship's movement influence can be found in Hackerott et al. (2018) and Santini et al. (2020). The wind speed sampled on a mobile platform can be corrected using Equation 2.

$$\vec{V}_{real} = T_{ae}\vec{V}_{obs} + T_{ae}\left(\vec{V}_t + \vec{w}\,\vec{r}\right) + \vec{V}_n \tag{2}$$

Where $\vec{V}_{real}$ is the real wind speed vector at the moment of measurement; $\vec{V}_{obs}$ is the speed measured by the anemometer; $\vec{V}_t$ and $\vec{w}$ are the angular and linear velocities of the measuring equipment itself, respectively; $\vec{V}_n$ is the ship's travel speed; $\vec{r}$ is the anemometer position vector in relation to the motion sensor and T_{ae} is the coordinate transformation matrix from the anemometer reference system to the earth coordinate system (x-axis, y-axis and z-axis).

According to Dong et al. (2021), the flux uncertainty from the motion correction procedure is less than 6%. There are a potential flux bias resulting from instrument calibration (gas analyzer, anemometer and meteorological sensors required to calculate air density: air temperature, relative humidity and pressure) is up to 4 %. The propagation bias for the imperfection calibration of each sensor can be up to 7%.

After the wind data correction, the turbulent flux calculations were performed by using the EddyPro - version 6.0 ® software (https://www.licor.com/eddypro) developed by LI-COR Environmental. We used the Webb Correction (Webb 1982) in order to minimize the moisture environmental interference in CO_2 data samples. In addition, this software was set to remove spurious values and to calculate the average flux in a 30-min window. Similar calculations based on EC were used in SW Atlantic for heat fluxes (Pezzi et al. 2016, Santini et al. 2020), momentum fluxes (Hackerott et al. 2018) and CO_2 fluxes (Oliveira et al. 2019, Pezzi et al. 2021). Recently Pezzi et al. (2021) showed these calculations for both heat and CO_2 fluxes over a warm core eddy in the SW Atlantic. A complementary variable used in this study is the friction velocity (u*). This variable gives us information about how turbulent the environment is (Arya 2001).

Satellite and reanalysis data

The satellite and reanalysis data set were used as auxiliary data to complement the understanding of the surface characteristics of the ocean's mesoscale and synoptic atmospheric conditions in the study region. The satellite data used in this study were: SST from the Multi-scale Ultra-high Resolution (MUR) with a spatial resolution of 1 km and daily temporal resolution. This study also used the Sea Surface Salinity (SSS) from the Soil Moisture – Ocean Salinity (SMOS) with daily temporal resolution and 0.25° spatial resolution and Chlorophyll (Chl) from Visible Infrared Imaging Radiometer Suite (VIIRS) sensor aboard the Suomi-NPP satellite (SNPP) with daily and 4 km of temporal and spatial resolutions. The Reanalysis derived data were the Sea Level Pressure (SLP), Air Temperature (T_{air}), and wind speed and direction were obtained from the European Centre for Medium-Range Weather Forecast (ECMWF) ERA5 (Hersbach et al. 2018). The ERA5 has the hourly temporal resolution with a 0.25° spatial resolution. More details are presented in Table II.

Table II. Satellite and reanalysis data used in this project, during the OP37, between 08 to 22 November 2018.

Variable	Data Source	Spatial resolution	Temporal resolution
Chlorophyll	VIIRS	4 km	Daily
Salinity	SMOS	0.25°	Daily
Sea Surface Temperature	MUR	1 km	Daily
Wind speed and direction	ERA 5	0.25°	Hourly
Sea Level Pressure	ERA 5	0.25°	Hourly

RESULTS AND DISCUSSION

The study region was split into two areas during H41 cruise, the DP and the BS, due to the different oceanic and atmospheric characteristics found between them. The CO_2 fluxes varied along the ship's route. Table III summarizes all data for the study region (DP, BS and total area). The CO_2 fluxes data were discarded under atmospheric stable conditions when the Monion-Obukhov stability parameter was greater than 0.2 (here, $\zeta > 0.2$). This is due to the inaccuracy in measuring turbulent fluxes when the turbulence is very small or intermittent (Sun et al. 2018, Yusup & Liu 2016, Pattey et al. 2002).

Our experiment was conducted during the Spring of 2018 (08 to 22 November 2018), which may have impacted on fluxes direction, and as a result both areas, DP and BS, acted on average as CO_2 sink. Those results agree the mean behavior for those areas for the entire season (Munro et al. 2015, Monteiro et al. 2020). However, the variability of the pCO_{2sw}, may affect the flux results during the season. The pCO_{2sw} at DP changes during the spring, as seen by Fay et al. (2018), where their values were higher at the beginning of the season. Munro found at DP, at the south of the PF, that the increasing pCO_{2sw} is slower than pCO_{2atm}, making this area a persistent CO_2 sink. The phytoplankton blooms typically occur at south of DP during spring (Carranza & Gille 2015). At the BS for late spring, photosynthesis decreases the CO_2 partial pressure in the surface seawater, enhancing ocean CO_2 uptake (Caetano et al. 2020).

The BS uptaked on average 38.59% more CO_2 than DP, as shown in Table III. This difference is attributed to the variability of both atmospheric and oceanic conditions along the H41's route. During the study period, the mean SST decreased from the DP towards BS (Figure 1 and Table III). The SSS data did not cover the entire area, there was just some data especially for the BS region. The Chl data also has gaps, due to clouds cover in this area during cruise period. These gaps are a result of how Chl is obtained, which is through a passive sensor that suffers interference from the clouds on its quality measurements. The BS presented more turbulence in the atmosphere boundary layer, with a maximum u* value of 0.9, allied to that the wind speed reached maximum value, 20.7 m s^{-1}.

The BS is characterized by colder waters than DP, which increases the CO_2 solubility and due the difference of partial pressure of carbon dioxide (ΔpCO_2) between ocean and atmosphere, that may direct the fluxes to the ocean. In addition, during the sampled period, the BS had a predominance of stable atmospheric conditions contributing to the region act as a CO_2 sink. The stability condition is observed in the marine atmospheric boundary layer (MABL), it is due to the difference between SST - T_{air} (Figure 3). The SST-T_{air} at the near-surface interface is an atmospheric stability parameter

Table III. Mean, maximum, and minimum values of the Ocean-atmosphere CO_2 fluxes (CO_2 Flux) (mmol $m^{-2}d^{-1}$); Sea Level Pressure (SLP) (hPa) (Air Pressure), Wind speed (m s^{-1}); and Friction velocity (u*) (m s^{-1}), Sea Surface Salinity (SSS); Sea Surface Temperature (SST) (°C); Chlorophyll-a concentration (chl) (mg m^{-3}); for the Drake Passage, Bransfield Strait and Total area. Values obtained along the ship track and the data were collected in the OP37 during the period of 08 to 22 November 2018.

		CO_2 flux	SLP	Wind speed	u*	SST-Tar	SSS	SST	chl
Drake Passage	mean	-1.70	980.94	15.48	0.33	-0.24	34.44	1.45	0.27
	max	21.38	993.40	20.29	0.56	2.47	36.98	5.31	0.64
	min	-11.46	967.35	1.30	0.08	-1.99	30.70	-0.76	0.10
Bransfield Strait	mean	-2.77	972.04	7.17	0.37	-1.21	35.11	-0.13	0.26
	max	47.84	994.35	20.73	0.90	1.70	35.38	0.32	0.41
	min	-41.05	953.08	1.00	0.08	-5.92	34.35	-0.76	0.19
Total area	mean	-2.49	973.22	9.27	0.36	-0.97	34.48	0.26	0.26
	max	47.84	994.35	20.73	0.90	2.47	36.98	5.31	0.64
	min	-41.05	953.08	1.00	0.08	-5.92	30.70	-0.76	0.10

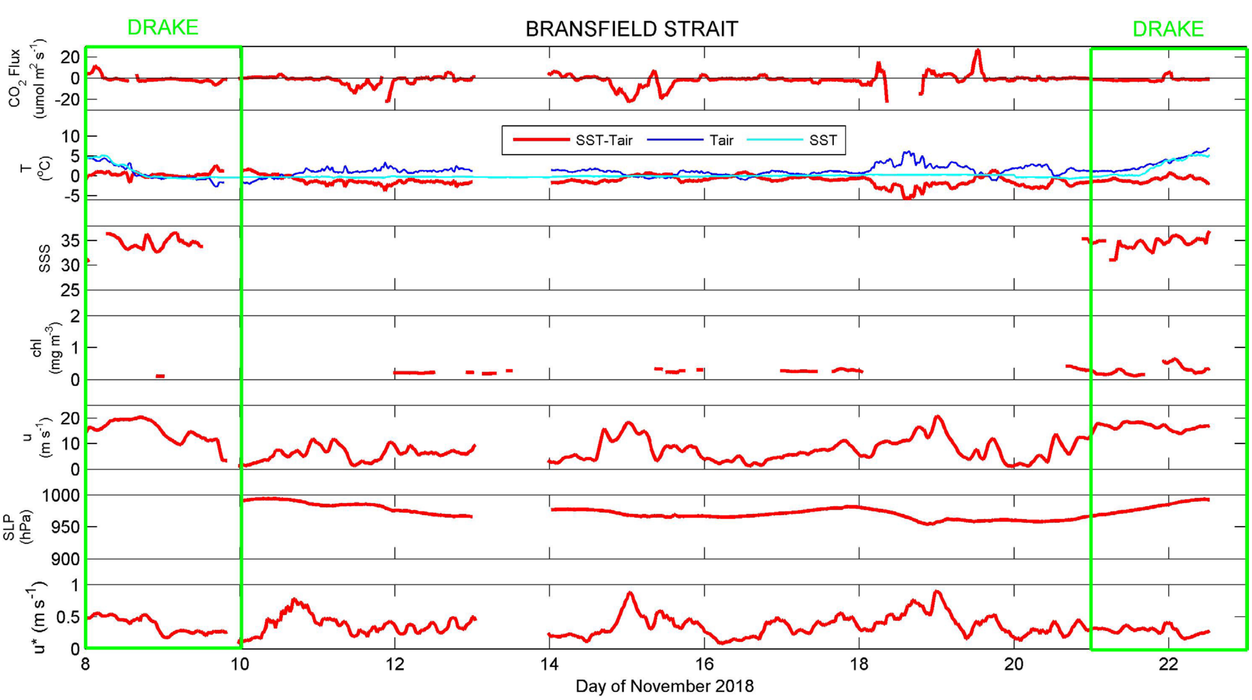

Figure 3. Time series of oceanographic and meteorological variables taken along the Po/V H41 route, from 08 to 22 November 2018. Ocean-atmosphere CO_2 fluxes (CO_2 Flux) (μmol$m^{-2}s^{-1}$); Sea Surface Temperature - air temperature (TSM-Tar) (°C), Sea Surface Temperature (SST), and Air temperature (Tair) (°C); Sea Surface Salinity (SSS); Chlorophyll-a concentration (chl) (mg m^{-3}); Wind speed (m s^{-1}); Sea Level Pressure (hPa) (SLP) and Friction velocity (u*) (m s^{-1}) The green rectangle separates the 2 areas: Drake Passage and Bransfield Strait.

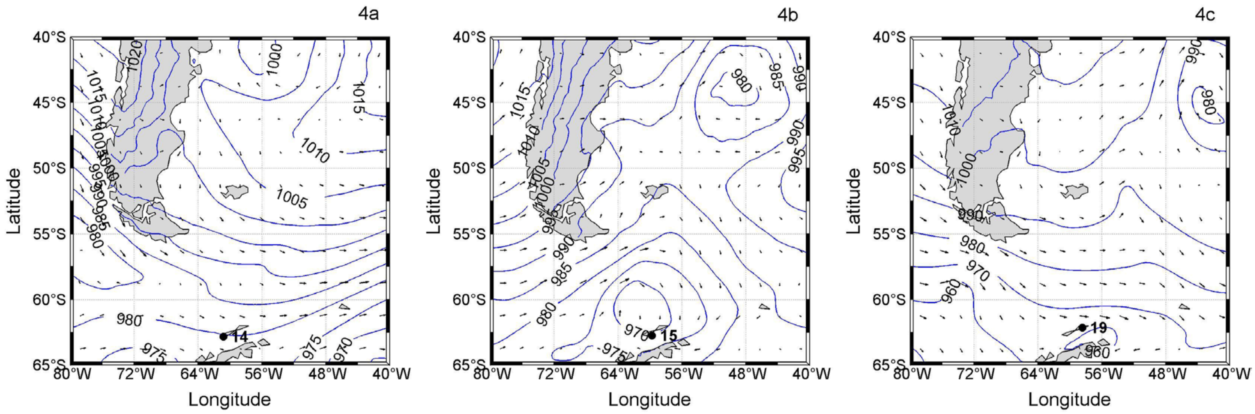

Figure 4. Sea mean level pressure (blue lines), wind direction (arrows) and Po/V H41 location (black point) during the days 14, 15 e 19 November 2018, 00H for each day. Data from Era5.

that indicates the preferential surface flux direction. When SST - T_{air} > 0, MABL is unstable, and when SST - Tair < 0, MABL is stable (Pezzi et al. 2005, 2009, 2016, De Camargo et al. 2013). Besides, during the ship's route, light to moderate rain occurred on some days. This rainfall allied to the influence of glacial meltwater dilution could reduce the salinity concentration in the ocean, also could induce the upwelling of nutrient-rich water supporting declines in pCO_{2sw} if light is not limiting for primary producers. The glacial meltwater inputs could influence in carbonate chemistry, by the dilution of carbonated ion concentration, so with a reduction of pCO_{2sw}. This condition, combined with colder waters that increase the ocean CO_2 solubility, could favors the CO_2 fluxes to be directed to the ocean. This result suggests the complexity of the factors controlling the spatial distribution of pCO_{2sw} in BS. Similar results were found by Ito et al. (2018), for this region. The authors also investigated the role played by surface waters in controlling the pCO_{2sw} and sea-air CO_2 fluxes in the Northern Antarctic Peninsula region. For the BS, during the Summer of 2009, the physical effects such as glacial meltwater discharges, oceanic fronts and eddies, thermodynamic effects and stratification of the mixing layer also modified the pCO_{2sw} variability. When considering the BS, the biological processes were responsible for the CO_2 sink in this area, but during 2009, the physical processes dominated, and the area was a weak source of CO_2. Caetano et al. (2020) suggested the temperature might cause significant variability in the ocean surface distribution of CO_2 over short shoreline distances in the Northern Antarctic Peninsula. During the period from 14 to 15 November 2018, the ship was near to a low pressure atmospheric system as seen in Figure 4a e 4b and produced strong winds at the surface (~ 17 m s^{-1}) as well as high-friction velocities (~ 0.8 m s^{-1}; Figure 3). These factors favored the vertical mass movement and the ocean surface mixing that driving the fluxes to the ocean. According to Wanninkhof & Triñanes (2017), the increase in wind speed affects the absorption of CO_2 by the oceans regardless of the direction of flow.

However, changes in pCO_{2sw} under the influence of glacial meltwater input in the BS region, could influence the CO_2 flux behavior. The glacial meltwater and sea-ice melting input modify the surface layer stability and favors the development of phytoplankton blooms (Varela et al. 2002). Changes in the salinity, derived from freshwater input, may cause the nitrate (NO3-) reduction caused by biological utilization reducing seawater alkalinity that has as consequence the increase of the pCO_{2sw} becoming sources of CO_2 (Takahashi et al. 2014) as observed some peaks on days of November 15, 18 and 19. Monteiro et al. (2020) found the Northern Antarctic Peninsula absorbed more CO_2 in the Spring and Summer than Autumn and Winter. Those authors showed in the Northern Antarctic Peninsula, in autumn and winter, upwelling events that increased the remineralized carbon in the sea surface, leading the region to act as a CO_2 source to the atmosphere. Furthermore, the peak on 19 November 2018, where the ocean acted as a source of CO_2, was due to a combination of some other factors: proximity of a low atmospheric pressure system, with approximately 950 ha (Figure 4c) and light to moderates surface winds (less than 10 m s^{-1}). Those factors contributed to the vertical movement in the MABL, thus decreasing CO_2 concentrations in the atmosphere near the ocean surface. As a result, the CO_2 fluxes were directed from ocean to atmosphere, with a mean value of 20 µmol m^{-2} s^{-1} (Figure 3). On the other days 10, 12, 16, 17 and 20 of November 2018, the CO_2 fluxes were near the neutrality, with a stable MABL and low turbulence, thus inhibiting the mass exchange at the ocean-atmosphere interface

The DP on average behaved as a sink of CO_2 as seen in Table III and Figure 5a. The main causes were associated with the colder SST (1.45 °C), and fresher (34.44) waters as seen in Table III. Thereby, the water properties such as SST and SSS had more impact on CO_2 fluxes compared to the presence of Chl, which had low concentration at DP. The Figure 5a shows in the south of the PF has acted as a CO_2 sink, due to the pCO_{2sw} being lower than the pCO_{2atm} (Munro et al. 2015), influenced by the cold and fresh water. However, the CO_2 fluxes at DP are less intense than at BS, due to the presence of the intense upwelling process around 60 – 65 °S, which increases remineralized carbon to the surface (Takahashi et al. 2012, Henley et al. 2020). The mean pCO_{2sw} for the DP was 368 µatm, value higher than as found by Fay et al. (2018), it was approximately 355 uatm in November of the period between 2002 and 2016, in DP. Similar results were found for Ito et al. (2018) in this region, for summer 2008. In their study which took place in the Northern Antarctic Peninsula and observed the role of surface water on controlling pCO_{2sw} and air CO_2 flux, the DP also presented a low concentration of Chl. However, in this study in the summer of 2008, DP acted as a source of CO_2. The surface Chl concentration is a proxy for the presence of primary production which has a role in the air-sea CO_2 fluxes as they may have a significant control on the gas partial pressure in the seawater (Monteiro et al. 2020, Henley et al. 2020). Song et al. (2015) discovered in their investigation the role of mesoscale eddies in modulating air-sea CO_2 flux in DP. In this study, the mesoscale eddies SST had a negative correlation with pCO_{2sw} in the ocean during the summer. Moreover, they highlighted that the dissolved inorganic carbon has more impact on CO_2 modulation than it does on temperature. However, Munro et al. (2015) reported the importance of the DP in the CO_2 sink for the SO during winter, especially in the south of the PF. Previous studies had reported the impacts of the SST and SSS on CO_2 fluxes, e.g., Woolf et al. (2016). And, found that SST has more considerable effects on the CO_2 ocean solubility (Woolf et al. 2016). This can may the main cause that led to less CO_2 assimilation by the ocean, at DP, where the warmer waters in this region produced less solubility of CO_2 in the ocean when compared to the BS.

At DP the ocean acted as a source of CO_2 to the atmosphere as seen in the CO_2 flux peaks during 8 and 22 of November 2018 (Figure 3 and 5a). Those days the ship was located at the north of the PF, that region has similar pCO_{2sw} and pCO_{2atm}, indicating near-neutral air-sea CO_2 flux or slight source to the atmosphere, those results are similar to the Munro et al. (2015) and Caetano et al. (2020). The pCO_{2sw} on the PF north was higher than to the south (Figure 5b), with mean values of 375 uatm, similar values found Ito et al. 2018. Moreover, this fact is also related to the unstable condition observed in

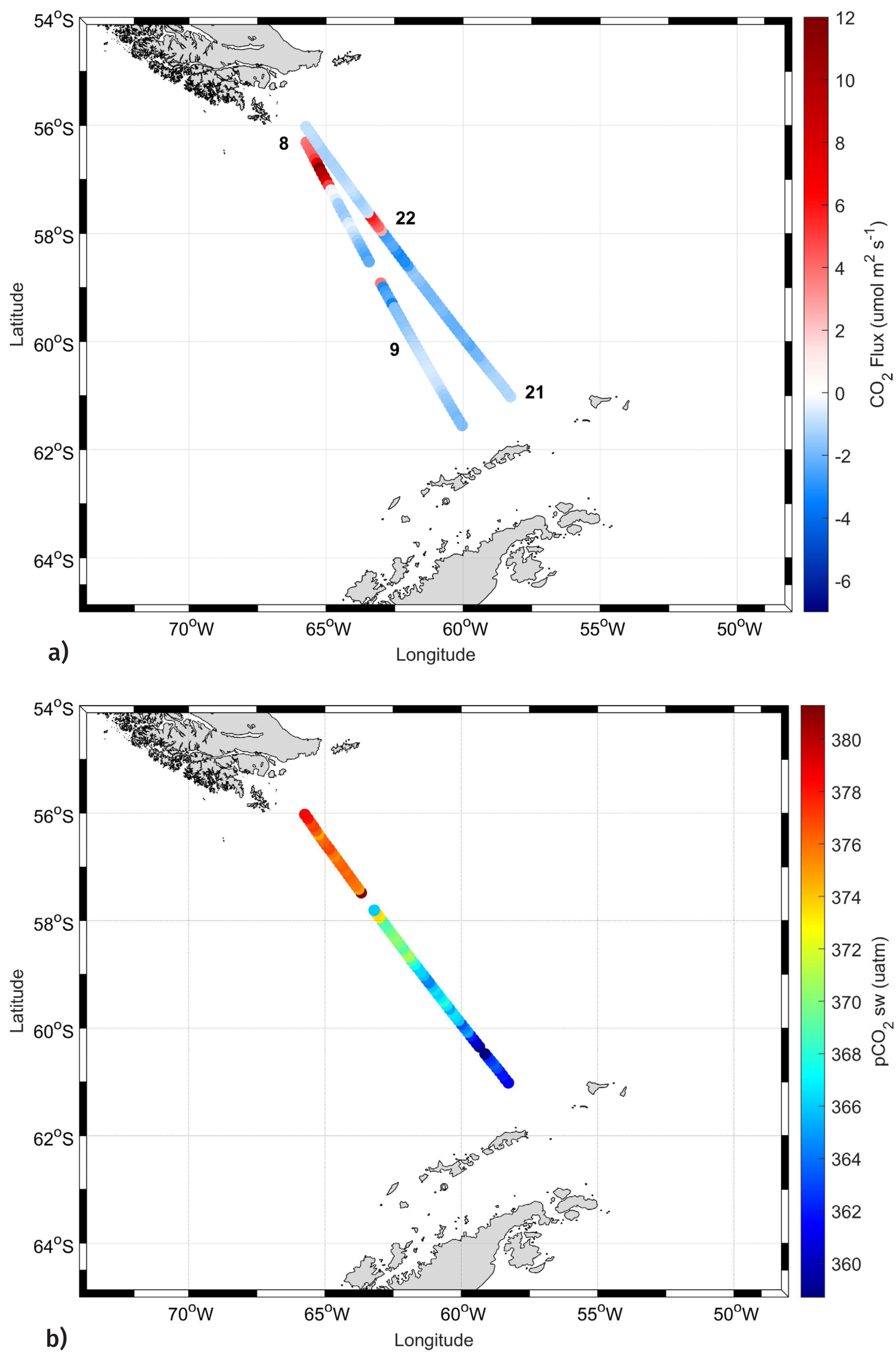

Figure 5. a) Ocean-atmosphere CO_2 fluxes (CO_2 Flux) ($\mu molm^{-2}s^{-1}$), and b) pCO_{2sw} (μatm) with Po/V H41 route at Drake Passage during the days 8, 9, 21 e 22 November 2018.

the MABL observed during those days produced an intensification of the wind speed at surface and above it within MABL vertical extension. Consequently, more turbulence was produced and shown by the u*, which favored the transfer of mass between the sea surface and the atmosphere (Wanninkhof & Triñanes, 2017). On the following days, 9 and 21 November 2018, when the ship was surveying over DP, the CO_2 fluxes were near to zero as seen in Figure 3 and 5a. In other words, there was no mass exchange between the ocean and the atmosphere. In this period, there was a predominance of low turbulence of less than 0.5 m s^{-1} (Figure 3), which inhibited the CO_2 fluxes.

The climate modes of variability, such as El Niño-Southern Oscillation (ENSO) and Southern Annular Mode (SAM), impact the variability of the surface carbonate system especially on interannual scale. During the November of 2018 the El niño was active and SAM was in a positive phase, in this case, some studies indicate more CO_2 uptake in the Northern Antarctic Peninsula (Brown et al. 2019, Costa et al. 2020). However, other studies have opposites results, they found that in the positive SAM phase the ocean acted as a CO_2 source due to the reduction in biological activities (Lovenduski et al. 2007; Leung et al. 2015). Another study did not find any effect of the SAM on the CO_2 carbon sink variability for 35 years (Keppler & Landschützer 2019). Our study period (8 to 22 November 2018) was conducted during a positive and active phase of the SAM and El Niño, and the area was a sink of CO_2. The results could have some influence of those climate modes of variability. However, it is difficult to address the sink CO_2 behavior in the area due to the climate modes of variability. The influence of ENSO and SAM changing the carbonate system parameters still not well understood in the scientific community.

CONCLUSIONS

This study showed the impacts of different atmospheric and oceanic conditions on the ocean-atmosphere CO_2 fluxes based on a combination of *in situ*, satellite, and reanalysis data sets. The *in situ* CO_2 fluxes data were collected in the DP and the BS in the second phase of OP37, covering the period from 8 to 22, November 2018. The CO_2 fluxes were obtained with the Eddy Covariance method (Miller et al. 2008, Pezzi et al. 2021). The synoptic oceanic conditions were analyzed with chlorophyll, SSS and SST from satellites. The atmospheric synoptic conditions were obtained through ERA5 reanalysis data set analyzing T_{air}, SLP, wind speed and direction.

The BS and DP behaved as CO_2 sinks on average, where the main cause was attributed to the colder water that intensified the CO_2 solubility in the ocean. Comparing the mean value of CO_2 fluxes, the BS uptaked on average 38.59% more CO_2 than DP. The DP, on average, behaved as a sink of CO_2 mainly due to physical characteristics. The south of the PF, DP has acted as a persistent CO_2 sink, due to the pCO_{2sw} being lower than the pCO_{2atm}, influenced by the cold and fresh water. However, the CO_2 fluxes at DP are less intense than at BS, due to the presence of the intense upwelling process around 60 – 65 °S, which increases remineralized carbon to the surface. There were some peaks of source of CO_2 in the north of the PF at DP, due to the unstable conditions of the atmosphere.

The BS was characterized by its colder waters compared to the DP, that contributes to the ocean act as sink. Furthermore, during the ship route, light to moderate rainfall was recorded in some days. This rainfall may have contributed to the reduction of salinity concentration in the ocean, thus decreasing pCO_{2sw}, directing the fluxes toward the ocean, or minimizing the CO_2 outgassing. In addition, during the sampled period, the BS had a predominance of stable atmospheric conditions contributing to the region act as a CO_2 sink. However, during the period there were some peaks of CO_2 source at BS, due to the reduction of seawater alkalinity by the glacial meltwater and sea-ice melting inputs, as consequence the increase of the pCO_{2sw}. Allied to that, the proximity of a low atmospheric pressure system and light to moderate turbulence and wind at the surface, thus it contributed to the vertical movement in the MABL.

This study supports the hypothesis that ocean-atmosphere CO_2 fluxes are highly dependent on oceanographic and meteorological conditions. This study also contributes to an improved understanding of the importance of the SO in the global carbon balance. The provided evidence shows that it is necessary to continue with observational campaigns in this region, to expand the knowledge about the SO's role in the global carbon dioxide cycle.

Acknowledgments

We thank the Brazilian Navy for making the cruise possible. We also thank the Brazilian Ministry of Science, Technology and Innovations (MCTI) and the Brazilian Antarctic Program (PROANTAR) for funding the ATMOS Project (CNPq/PROANTAR 443013/2018-7). L.P.P. is partly funded through a Conselho Nacional de Desenvolvimento Científico e Tecnológico (CNPq) Scientific Productivity Fellowship (CNPq/304858/2019-6). This study was financed in part by the Coordenação de Aperfeiçoamento de Pessoal de Nível Superior - Brasil (CAPES) - Finance Code 001.

REFERENCES

ARYA SP. 2001. Introduction to micrometeorology, 2nd ed., USA: Academic Press, 420 p.

BARLLET EMR, TOSONOTTO GV, PIOLA A, SIERRA ME & MATA MM. 2018. On the temporal variability of intermediate and deep waters in the Western Basin of the Bransfield Strait. March 2018. Deep Sea Res Part II 149: 31-46.

BENALLAL MA, MOUSSA H, LENCINA-AVILA JM, TOURATIER F, GOYET C, EL JAI MC, POISSON M & POISSON A. 2017. Satellite-derived CO2 flux in the surface seawater of the Austral Ocean south of Australia. Int J Remote Sens 38(6): 1600-1625.

BIANCHI AA, HERNÁN DRP, PERLENDER GI, OSIROFF AP, SEGURA V, LUTZ V, CLARA ML, BALESTRIN CF & PIOLA AR. 2009. Annual balance and seasonal variability of sea-air CO2 fluxes in the Patagonia Sea: Their relationship with fronts and chlorophyll distribution. J Geophys Res 114: C03018.

BROWN MS, MUNRO DR, FEEHAN CJ, SWEENEY C, DUCKLOW HW & SCHOFIELD OM. 2019. Enhanced oceanic CO2 uptake along the rapidly changing West Antarctic Peninsula. Nat Clim Change 9: 678-683.

CAETANO LS, POLLERY RCG, KERR R, MAGRANI F, NETO AA, VIEIRA R & MAROTTA H. 2020. High-resolution spatial distribution of p CO2 in the coastal Southern Ocean in late spring. Antarct Sci 32(6): 476-485.

CAMPBELL SCIENTIFIC INC. 2016. IRGASON integrated CO2 and H2O open-path gas analyzer and 3-D sonic anemometer. Instruction Manual, 72 p.

CANADELL JG, LE QUÉRÉ C, RAUPACH MR, FIELD CB, BUITENHUIS ET, CIAIS P, CONWAY TJ, GILLETT NP, HOUGHTON RA & MARLAND G. 2007. Contributions to accelerating atmospheric CO2 growth from economic activity, carbon intensity, and efficiency of natural sinks. Proc Natl Acad Sci U S A 104(47): 18866-18870.

CARRANZA MM & GILLE ST. 2015. Southern Ocean wind-driven entrainment enhances satellite chlorophyll-a through the summer. J Geophys Res Oceans 120: 304-323.

COSTA RR ET AL. 2020. Dynamics of an intense diatom bloom in the Northern Antarctic Peninsula, February 2016. Limnol Oceanogr 65(9): 1-20.

DE CAMARGO R, TODESCO E, PEZZI LP & DE SOUZA RB. 2013. Modulation mechanisms of marine atmospheric boundary layer at the Brazil-Malvinas Confluence region. J Geophy Res Atmos 118(12): 6266-6280.

DONG Y, YANG M, BAKKER DCE, KITIDIS V, & BELL TG. 2021. Uncertainties in eddy covariance air-sea CO2 flux measurements and implications for gas transfer velocity parameterisations. Atmos Chem Phys 21(10): 8089- 8110.

EDSON JB, HINTON AA, PRADA KE, HARE JE & FAIRALL CW. 1998. Direct covariance flux estimates from mobile platforms at sea. J Atmos Ocean Technol 15(2): 547-562.

FAY AR, LOVENDUSKI NS, MCKINLEY GA, MUNRO DR, SWEENEY C, GRAY AR, LANDSCHÜTZER P, STEPHENS BB, TAKAHASHI T & WILLIAMS N. 2018. Utilizing the Drake Passage time-series to understand variability and change in subpolar Southern Ocean pCO2. Biogeosciences 15: 3841-3855.

FRATINI F, IBROM A, ARRIGA N, BURBA G & PAPALE D. 2012. Relative humidity effects of water vapour fluxes measured with closed-path eddy-covariance systems with short sampling lines. Agric For Meteorol 165: 53-63.

FOKEN T, GÖOCKEDE M, MAUDER M, MAHRT L, AMIRO B & MUNGER W. 2005. Post-field data quality control. Dordrecht, Netherlands: Springer, 181-208 p.

FRÖLICHER TL, SARMIENTO JL, PAYNTER DJ, DUNNE JP, KRASTING JP & WINTON M. 2015. Dominance of the Southern Ocean in Anthropogenic Carbon and Heat Uptake in CMIP5 Model. J Clim 28(2): 862-886.

FUJITANI T. 1981. Direct measurement of turbulent fluxes over the sea during AMTEX. Pap Meteorol Geophys 32(3): 119-134.

HACKEROTT JA, PEZZI LP, BAKHODAY PASKYABI M, OLIVEIRA AP, REUDER J, DE SOUZA RB & DE CAMARGO R. 2018. The Role of Roughness and Stability on the Momentum Flux in the Marine Atmospheric Surface Layer: A Study on the Southwestern Atlantic Ocean. J Geophys Res Atmos 123(8): 3914-3932.

HENLEY SF ET AL. 2019. Variability and change in the west Antarctic Peninsula marine system: Research priorities and opportunities. Prog Oceanogr 173: 208-237.

HENLEY SF ET AL. 2020. Changing biogeochemistry of the Southern Ocean and its ecosystem implications. Front Mar Sci 7: 581.

HERSBACH H ET AL. 2018. ERA5 hourly data on single levels from 1979 to present. Copernicus Climate Change Service (C3S) Climate Data Store (CDS).

IPCC. 2021. Climate Change 2021: The Physical Science Basis. Contribution of Working Group I to the Sixth Assessment Report of the Intergovernmental Panel on Climate Change. In: Masson-Delmotte V et al. (Eds), Cambridge University Press. In Press.

ITO RG, TAVANO VM, MENDES CRB & GARCIA CAE. 2018. Sea-air CO2 fluxes and pCO2 variability in the Northern Antarctic Peninsula during three summer periods (2008-2010). Deep Res Part II Top Stud Oceanogr 149: 84-98.

JIANG C, GILLE ST, SPRINTALL J & SWEENEY C. 2014. Drake Passage Oceanic pCO2: Evaluating CMIP5 Coupled Carbon-Climate Models Using in situ Observations. J Clim 27(1): 76-100.

KEPPLER L & LANDSCHÜTZER P. 2019. Regional wind variability modulates the Southern Ocean carbon sink. Sci Rep 9(1): 1-10.

LENCINA AVILA JM ET AL. 2018. Past and future evolution of the marine carbonate system in a coastal zone of the Northern Antarctic Peninsula. Deep Res. Part II Top Stud. Oceanogr 149: 193-205.

LE QUÉRÉ C, TAKAHASHI T, BUITENHUIS ET, RÖDENBECK C & SUTHERLAND SC. 2010. Impact of climate change and variability on the global oceanic sink of CO2. Glob Biogeochem Cycles 24: GB4007.

LE QUÉRÉ C ET AL. 2016. Global Carbon Budget 2016. Earth Syst Sci Data 8: 605-649.

LE QUÉRÉ C ET AL. 2018. Global Carbon Budget 2018. Earth Syst Sci Data 10: 2141-2194.

LEUNG S, CABRÉ A & MARINOV I. 2015. A latitudinally banded phytoplankton response to 21st century climate change in the Southern Ocean across the CMIP5 model suite. Biogeosciences 12: 5715-5734.

LOPEZ O, GARCIA MA, GOMIS D, ROJAS P, SOSPEDRA J & ARCILLA-SÁNCHEZ A. 1999. Hydrographic and hydrodynamic characteristics a of the eastern basin of the Bransfiled Strait. Deep Sea Res Part I Oceanogr Res Pap 46: 1755-1778.

LOHRENZ SE, CAI WJ, CHAKRABORTY S, HUANG WJ, GUO X, HE R, XUE Z, FENNEL K, HOWDEN S & TIAN H. 2018. Satellite estimation of coastal pCO2 and air-sea flux of carbon dioxide in the northern Gulf of Mexico. Remote Sens Environ 207: 71-83.

LANDSCHÜTZER P, GRUBER N, BAKKER D & SCHUSTER U. 2014. Recent variability of the global ocean carbon sink. Glob Biogeochem Cycles 28 (9): 927-949.

LOVENDUSKI NS, GRUBER N, DONEY SC & LIMA ID. 2007. Enhanced CO2 outgassing in the Southern Ocean from a positive phase of the Southern annular mode. Glob Biogeochem Cycles 21: GB2026.

LOVENDUSKI NS, LONG MC, GENT PR & LINDSAY K. 2013. Multi-decadal trends in the advection and mixing of natural carbon in the Southern Ocean. Geophys Res Lett 40: 139-142.

LOVENDUSKI NS, LONG MC & LINDSAY K. 2015. Natural variability in the surface ocean carbonate ion concentration. Biogeosciences 12(21): 6321-6335.

MAJKUT JD, SARMIENTO JL & RODGERS KB. 2014. A growing oceanic carbon uptake: Results from an inversion study of surface *p*CO2 data. Glob Biogeochem Cycles 28: 335-351.

METZL N. 2009. Decadal increase of oceanic carbon dioxide in the Southern Indian Ocean surface waters (1991-2007). Deep-Sea Res II 56: 607-619.

MILLER SD, HRISTOV TS, EDSON JB & FRIEHE CA. 2008. Platform motion effects on measurements of turbulence and air-sea exchange over the open ocean. J Atmos Ocean Technol 25(9): 1683-1694.

MONTEIRO T, KERR R & MACHADO C. 2020. Seasonal variability of net sea-air CO2 fluxes in a coastal region of the Northern Antarctic Peninsula. Sci Rep (0123456789): 1-15.

MUNRO DR, LOVENDUSKI NS, STEPHENS BB, NEWBERGER T, ARRIGO KR, TAKAHASHI T, QUAY PD, SPRINTALL J, FREEMAN MN & SWEENEY C. 2015. Estimates of net community production in the Southern Ocean determined from time series observations (2002-2011) of nutrients, dissolved inorganic carbon, and surface ocean *p*CO2 in Drake Passage. Deep-Sea Res II 114: 49-63.

NOAA - NATIONAL CENTERS FOR ENVIRONMENTAL INFORMATION. 2019. Climate at a Glance: Global Time Series, from https://www.ncdc.noaa.gov/cag/.

OGUNDARE MO, FRANSSON A, CHIERICI M, JOUBERT WR & ROYCHOUDHURY AN. 2021. Variability of Sea-Air Carbon Dioxide Flux in Autumn Across the Weddell Gyre and Offshore Dronning Maud Land in the Southern Ocean. Front Mar Sci 7: 1168.

OLIVEIRA RR, PEZZI LP, SOUZA RB, SANTINI MF, CUNHA LC & PACHECO FS. 2019. First measurements of the ocean-atmosphere CO2 fluxes at the Cabo Frio upwelling system region, Southwestern Atlantic Ocean. Cont Shelf Res 181(April): 135-142.

ORSELLI IBM, KERR R, ITO RG, TAVANO VM, MENDES CRB & GARCIA CAE. 2017. How fast is the Patagonian shelf-break acidifying? J Mar Syst 178: 1-14.

ORSI HA, WHITWORTH T & WORTH DN. 1995. On the meridional extent and fronts of the Antarctic Circumpolar Current. Deep Res I 42(5): 641-673.

PARDO PC, PÉREZ FF, KHATIWALA S & RÍOS AF. 2014. Anthropogenic CO2 estimates in the Southern Ocean: Storage partitioning in the different water masses. Prog Oceanogr 120: 230-242.

PATTEY E, STRACHAN IB, DESJARDINS RL & MASSHEDER J. 2002. Measuring nighttime CO2 flux over terrestrial ecosystems using eddy covariance and nocturnal boundary layer methods. Agric For Meteorol 113(1-4): 145-158.

PEZZI LP, DE SOUZA, RB, ACEVEDO O, WAINER I, MATA MM, GARCIA CAE & DE CAMARGO R. 2009. Multiyear measurements of the oceanic and atmospheric boundary layers at the Brazil-Malvinas confluence region. J Geophys Res Atmos 114(19): 1-19.

PEZZI LP, SOUZA RB, SANTINI MF & MILLER AJ. 2021. Oceanic eddy-induced modifications on the air-sea heat and CO2 fluxes in the Brazil-Malvinas Confluence. Sci Rep 11: 10648.

PEZZI LP, SOUZA RB, DOURADO MS, GARCIA CAE, MATA MM & SILVA-DIAS MAF. 2005. Ocean-atmosphere in situ observations at the Brazil-Malvinas Confluence region. Geophys Res Lett 32(22): 1-4.

PEZZI LP, SOUZA RB, FARIAS PC, ACEVEDO O & MILLER AJ. 2016. Air-sea interaction at the Southern Brazilian Continental Shelf: In situ observations. J Geophys Res Ocean 121(9): 6671-6695.

RINTOUL S, HUGHES C & OLBERS D. 2001. Chapter 4.6 The Antarctic Circumpolar Current system. In: Siedler G, Church J & Gould J (Eds), Ocean circulation and climate; observing and modelling the global ocean. Int Geophys Series, Academic Press, p. 271-302.

RODEN NP, TILBROOK B, TRULL TW, VIRTUE P & WILLIAMS GD. 2016. Carbon cycling dynamics in the seasonal sea-ice zone of East Antarctica. J Geophys Res Oceans 121: 8749-8769.

SANTINI MF, SOUZA RB, PEZZI LP & SWART S. 2020. Observations of air - sea heat fluxes in the southwestern Atlantic under high-frequency ocean and atmospheric perturbations. Q J R Meteorol Soc 146: 4226-4251.

SATO OT. 2005. Fluxos de calor oceânico medido por meio de satélites. In: Souza RB (Ed), Oceanografia por Satélites. São Paulo, Brasil: Oficina de Texto, p. 148-165.

SONG H, MARSHALL J, MUNRO DR, DUTKIEWICZ S, SWEENEY C, MCGILLICUDDY DJ & HAUSMANN U. 2016. Mesoscale modulation of air-sea CO2 flux in Drake Passage. J Geophys Res Oceans 121: 6635-6649.

SOUZA R, PEZZI L, SWART S, OLIVEIRA F & SANTINI M. 2021. Air-Sea Interactions over Eddies in the Brazil-Malvinas Confluence. Remote Sens 13(7): 1335.

SUN Y, JIA L, CHEN Q & ZHENG C. 2018. Optimizing window length for turbulent heat flux calculations from airborne eddy covariance measurements under near neutral to unstable atmospheric stability conditions. Remote Sens 10(5).

SHUTLER J, LAND P, PIOLLE JF, WOOLF DK, GODDIJN-MURPHY L, PAUL F, DONLON C, GIRARD-ARDHUIN F, CHAPRON B & DONLON CG. 2016. FluxEngine: A flexible processing system for calculating atmosphere-ocean carbon dioxide gas fluxes and climatologies. J Atmos Ocean Technol 33(4): 741-756.

STEPHENSON GR, GILLE ST & SPRINTALL J. 2012. Seasonal variability of upper ocean heat content in Drake Passage. J Geophys Res 117: C04019.

STULL RB. 1988. An introduction to boundary layer meteorology. Dordrecht: Kluwer Academic Publishers, Dordrecht, Boston and London, 666 p.

SWART S ET AL. 2019. Constraining Southern Ocean air-sea ice fluxes through enhanced observations. Front Mar Sci 6: 1-10.

TAKAHASHI T ET AL. 2009. Climatological mean and decadal change in surface ocean *p*CO2, and net sea-air CO2 flux over the global oceans. Deep Res Part II Top Stud Oceanogr 56(8-10): 554-577.

TAKAHASHI T, SWEENEY C, HALES B, CHIPMAN DW, NEWBERGER T, GODDARD JG, IANNUZZI RA & SUTHERLAND SC. 2012. The changing carbon cycle in the Southern Ocean. Oceanography 25(3): 26-37.

TAKAHASHI T, SUTHERLAND SC, CHIPMAN DW, GODDARD JG, HO C, NEWBERGER T, SWEENEY C & MUNRO DR. 2014. Climatological distributions of pH, pCO2, total CO2, alkalinity, and CaCO3 saturation in the global surface ocean, and temporal changes at selected locations. Mar Chem 164: 95-125.

TRENBERTH KE, FASULLO JT & KIEHL J. 2009. Earth's global energy budget. Bull Am Meteorol Soc 90(3): 311-323.

VARELA M, FERNANDEZ E & SERRET P. 2002. Size-fractionated phytoplankton biomass and primary production in the Gerlache and south Bransfield Straits (Antarctic Peninsula) in Austral summer 1995-1996. Deep Sea Res Part II: Topical Studies in Oceanography 49(4-5): 749-768.

WANNINKHOF R & TRIÑANES J. 2017. The impact of changing wind speeds on gas transfer and its effect on global air-sea CO2 fluxes. Global Biogeochem Cycles 31(6): 961-974.

WEBB EK. 1982. On the correction of flux measurements for effects of heat and water vapour transfer. Boundary-Layer Meteorol 23(2): 251-254.

WOOLF DK, LAND PE, SHUTLER JD, GODDIJN-MURPHY LM & DONLON CJ. 2016. On the calculation of air-sea fluxes of CO2 in the presence of temperature and salinity gradients. J Geophys Res Ocean 121(2): 1229-1248.

XUE L, GAO L, CAI WJ, YU W & WEI M. 2015. Response of sea surface fugacity of CO2 to the SAM shift south of Tasmania: Regional differences. Geophys Res Lett 42: 3973-3979.

YUSUP Y & LIU H. 2016. Effects of atmospheric surface layer stability on turbulent fluxes of heat and water vapor across the water-atmosphere interface. J Hydrometeorol 17(11): 2835-2851.

ZHOU M, NIILER PP & HU JH. 2002. Surface currents in the Bransfield and Gerlache Straits, Antarctica. Deep Res Part I Oceanogr Res Pap 49(2): 267-280.

Manuscript received on July 27, 2022;
accepted for publication on October 8, 2022

CELINA CÂNDIDA F. RODRIGUES[1]
https://orcid.org/0000-0002-6872-1977

MARCELO F. SANTINI[1]
https://orcid.org/0000-0002-6760-2247

LUCIANA S. LIMA[1]
https://orcid.org/0000-0001-7988-0853

UESLEI ADRIANO SUTIL[1]
https://orcid.org/0000-0002-7150-536X

JONAS T. CARVALHO[1]
https://orcid.org/0000-0002-1225-3457

MYLENE JEAN CABRERA[1]
https://orcid.org/0000-0002-4577-8743

ELIANA B. ROSA[1]
https://orcid.org/0000-0002-2021-3789

JACOB W. BURNS[2]
https://orcid.org/0000-0003-4334-4762

LUCIANO P. PEZZI[1]
https://orcid.org/0000-0001-6016-4320

[1]National Institute for Space Research (INPE), Laboratory of Ocean and Atmosphere Studies (LOA), Earth Observation and Geoinformatics Division (OBT), Av. dos Astronautas, 1758, Jardim da Granja, 12227-010 São José dos Campos, SP, Brazil

[2]University of Kansas, Center for Remote Sensing of Ice Sheets (CReSIS), National Science Foundation (NSF), 2335 Irving Hill Road, Lawrence, 66045, Kansas, USA

Correspondence to: **Celina Cândida Ferreira Rodrigues**
E-mail: celina.rodrigues@inpe.br

Author contributions

CCFR, LPP and MFS conceived this study. CCFR conducted the data process, data analysis and wrote most of the manuscript.; LPP and MFS, corrected the manuscript. MSF, MJC, EBR and UAS were on board and collected the data during OP37. LSL, MJC, EBR, UAS, JTC AND JWB participated in the discussion and provided suggestions on the study format.